Time-Resolved Dynamics of the OH Stretching Vibration in Aqueous NaCl Hydrate

Stanislav Pandelov, Bert M. Pilles, Jasper C. Werhahn, and Hristo Iglev*

Physik-Department E11, Technische Universität München, D-85748 Garching, Germany

Received: May 15, 2009; Revised Manuscript Received: June 29, 2009

We report on the first time-resolved study of the OH stretching vibration in NaCl dihydrate with the use of two-color IR spectroscopy. The sample is characterized by conventional FTIR spectroscopy. The water molecules bound in the hydrate show two well separated absorption bands at 3426 cm^{-1} and 3541 cm^{-1}. The transient data display an ultrafast heating of the polycrystalline ice−hydrate samples after excitation of the OH stretching vibration and its transient relaxation. The relaxation time of the low-frequency OH stretching band in the NaCl hydrate is measured to be 6.8 ± 1 ps. The dynamics are significantly slower than those measured in neat water. This fact, together with the reproducible crystalline environment reveals the potential of aqueous hydrates for a systematic investigation of the OH stretching vibration in varying hydrogen bonding environments.

Introduction

The hydrogen bond is ubiquitous in life sciences, since it is responsible for the anomalies of water, without which life would not have developed on this planet. Therefore, the H bond has attracted continuous scientific interest.[1−6] Nevertheless, its nature is not fully understood. The observed dynamics of H-bonds occur on time scales ranging from femtoseconds to several picoseconds, reflecting the motion of single water molecules up to diffusive motions of several molecules.[7] The corresponding intermolecular vibrations show up in a spectral range that is not easily accessible experimentally and overlaps with other low-frequency modes.[4] To overcome this limitation, the H-bonding network is often probed indirectly by utilizing the OH stretching vibration.[7−14]

The IR absorption spectrum of the OH stretch in liquid water consists of a broad band centered around 3400 cm^{-1}, as compared to the gas phase value of 3700 cm^{-1}. It is commonly accepted that the amount of red shift of the vibration corresponds to the strength of the according H-bond.[4,5] It is still heavily discussed whether the broad distribution of OH stretch frequencies represents a manifold of more or less discrete environments of the observed molecules[9,15,16] or whether the broadening of the band stems from stochastically distributed H-bond strengths without preferred local substructures.[12,17]

Structural investigations in water have been performed with NMR,[18] X-ray,[19] and neutron diffraction.[20−22] However, the limited time resolution in this type of experiment hindered the direct correlation between the derived structure information and the fast relaxation dynamics observed in femtosecond IR spectroscopy. The rapidity of the involved processes requires high temporal resolution. The ultrashort pulses used to resolve the processes in the time domain excited almost the whole OH stretch band simultaneously, thus inhibiting the determination of the frequency dependent relaxation pathways.[23] More sophisticated experiments like three-pulse photon echo have been employed[12,24,25] to obtain complementary information, but again the interpretation and the linking to structural information prove to be very difficult. Comparison with other model systems with a more clearly defined structure and slower dynamics appears to be advantageous.

Another key question concerning the aqueous hydrogen bond network is the process of solvation. Charged or polar particles are solvated in water and interact with their aqueous surroundings in an H-bond like manner. The dynamics of the aqueous environment change dramatically due to the interaction with the solute.[26−29] The studied OH stretching vibrations lying in the same spectral range can either be located in the vicinity of the cations or anions or be spatially separated from the solvated particles, possessing different relaxation dynamics. Theoretical work can faciliate the structural interpretation.[30−32] Structure and dynamics of the H-bonded network in the bulk can be assessed by means of classical, semiclassical and first-principles models,[33−36] the accuracy of the calculations being in principle only limited by computational power available. Still, the connection between the theoretical trajectories and experimentally accessible values, such as spectroscopic data is not fully clarified.[15] Dynamical spectroscopical information proves to be hard to be predicted theoretically,[37,38] yet it represents an important source of experimental information. The recently developed molecular dynamics potential TTM3-F[39] is capable of predicting the steady-state spectrum of liquid water accurately, at the same time reproducing the geometry of the water molecules in the respective phase.[40]

Here we want to propose a model system that seems helpful to overcome some of the mentioned problems. Solid hydrates of inorganic salts have attracted special interest due to their importance in geology, chemistry, and physics.[41−43] Salt hydrates offer an enormous variety of aqueous H-bond environments with varying bonding partners and distances.[43] Thus they serve as ideal benchmark systems to study the spectral signature of the water molecule in different environments.

The crystal structure and the absorption spectra of most hydrates have been measured previously.[4,46] The measurements allowed to correlate the geometric properties of the hydrogen bond (intra- and intermolecular bond lengths) to the frequency shift of the OH stretching vibration.[44] This correlation between bond length and strength is rather intuitive and has been established very early in the literature,[5] and due to the crystalline structure of the hydrates the spectral signature and geometry of

* Corresponding author. E-mail: higlev@ph.tum.de.

10.1021/jp904558m CCC: $40.75
Published on Web 09/01/2009

the hydrogen bond was easily accessible in this system, making it an ideal candidate for these studies. These linear techniques have already delivered a wealth of information on the properties of the hydrogen bond. Yet, examination with nonlinear techniques has, to the best of our knowledge, not been attempted, probably due to difficulties in the preparation of suitable monocrystals. In this work, we investigate the spectral signature of isotopically diluted OH groups in NaCl−hydrate with time-resolved infrared pump−probe spectroscopy. The crystalline ordering allows an accurate correlation of new transient spectral and structural data. Moreover, the crystal structure faciliates the theoretical description of these systems, making calculations of the spectra and dynamics feasible.

Experimental Section

Steady-state infrared absorption spectra of the samples discussed below were obtained from a commercial VECTOR 22 Fourier-transform infrared spectrometer (FTIR, Bruker Optics) with a spectral resolution of 1 cm^{-1}. To overcome the problem induced by the different temperature dependence of the symmetric and antisymmetric stretching vibrations of pure H_2O, we used 15 M HDO in D_2O samples. The HDO concentration is chosen in a way to allow sufficient energy deposition for the time-resolved measurements, yet maintain a relatively small H_2O concentration in the sample. The solvent was prepared by isotopic exchange in a mixture of appropriate amounts of D_2O (>99.9 atom % D) and tridistilled H_2O. Here we investigate aqueous solutions of LiCl, NaCl, and KCl (Merck Eurolab, GR, for analysis) at concentrations close to saturation. The polycrystalline hydrate samples are grown by slowly cooling the salt solution between two CaF_2 windows with a 3.5 μm spacer in a cryostat to 180 K at ambient pressure and warming it up again to the desired temperature later on.

The picosecond infrared spectrometer used for the time-resolved measurements has been described elsewhere.[45] The laser system provides IR pulses tunable in the range 1700−3700 cm^{-1} (2300−3700 cm^{-1}) with duration of 0.8 ps (1 ps), spectral width of 24 cm^{-1} (19 cm^{-1}), and typical energies of 10 nJ (7 μJ). Numbers in parentheses refer to the pump pulses. The repetition rate of the laser system is 43 Hz. The probe beam diameter in the sample of approximately 75 μm is a factor two smaller than that of the pump beam, so that only the central part of the interaction volume with maximum excitation is monitored. The energy transmission $T(\nu)$ of the probing pulse through the excited sample is measured for perpendicular polarization with respect to the linear polarization of the pump beam and compared with the probe transmittance $T_0(\nu)$ for blocked excitation beam. The absorption change, defined as $\Delta OD(\nu) = -\log(T(\nu)/T_0(\nu))$, is plotted in the figures.

FTIR Spectroscopy

Prior to the pump probe measurements, the investigated samples are characterized by conventional infrared spectroscopy. This method has been employed successfully before to characterize various hydrates.[46,47] The absorption spectrum measured in the region of the OH stretching vibration is presented in Figure 1B−D for three salt−HDO:D_2O mixtures. The spectra are shown for two sample temperatures of 275 K (red dashed lines) and 200 K (blue solid lines) in the liquid and solid phase, respectively. The well-known signature of the OH stretching band of the pure solvent (15 M HDO in D_2O) is shown in Figure 1A for comparison. The two phases are readily distinguished. This makes time-resolved IR spectroscopy an appropriate tool for studying ultrafast solid−liquid phase transitions of hydrogen bonded systems.

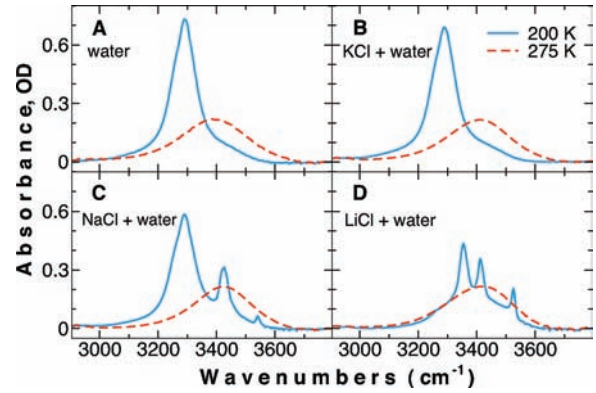

Figure 1. FTIR spectra of various aqueous HDO:D_2O (15 M) solutions (see inset). The samples are measured in the liquid (275 K, red dashed lines) and in the solid phase (200 K, blue solid lines).

Figure 1B shows the infrared absorption spectrum for aqueous electrolytes where no hydrate formation takes place. The OH stretch peak of the liquid KCl solution is slightly shifted due to the high concentration of ions that alter the hydrogen bond network,[29] while the spectral signature of the solid phase is almost identical to that of pure ice. No spectral changes occur upon freezing, since the salt precipitates and pure ice is formed.

The shape of the OH absorption band changes significantly upon hydrate formation, as shown for the NaCl hydrate in Figure 1C. Sharp peaks emerge in the OH spectral region that indicate the crystalline H-bonding arrangement. Due to the limited solubility of NaCl the ice band is also found here, since ice crystals form along with the hydrate. These crystal components, however, are spatially separated. Here, it should be noted that the absorption amplitude measured at 3290 cm^{-1} is smaller compared to the corresponding value in Figure 1A for the same sample thickness, since part of the water molecules are bound in the hydrate crystal. Figure 1D shows an example for the group of highly solvable salts such as LiCl, characterized by the absence of the well-defined ice peak in the OH stretching band.

For the interpretation of the time-resolved data (see below) measured in a polycrystalline hydrate structure of NaCl HDO:D_2O (15 M), a detailed analysis of the convectional spectrum is required. Figure 2A shows that the FTIR spectrum of the sample (black solid curve) can be represented by the sum of two Lorentz peaks (green dash-dotted line) and one steady-state ice spectrum (blue dashed line). It can be seen that the calculated curve (red dotted line) reproduces the measured band structure very well. Here, the spectrum of the ice phase is calculated by scaling the absorption of pure HDO:D_2O (15 M) at the same temperature (see Figure 1A). The scaling factor of 0.8 contains information about the fraction of water molecules bound in the hydrate lattice. Taking into account the NaCl concentration of 5.5 M in the sample, the structure is calculated to be a dihydrate, which is the only one reported in the literature.[48]

The Lorentz peaks in Figure 2A are fitted numerically and are attributed to the OH stretching vibrations of water molecules bound in the hydrate crystal. The extracted positions of the two hydrate bands are 3426 and 3541 cm^{-1}, respectively. The spectral width of the latter is 18 cm^{-1} and is a factor of 2 smaller than that of the stronger hydrate mode at 3426 cm^{-1} (34 cm^{-1}). The sharp spectral signature of both vibrations supports the assumption that the water molecules are in crystalline phase.

The temperature dependence of the IR spectrum of the ice−hydrate mixture is shown in Figure 2B. The spectrum of

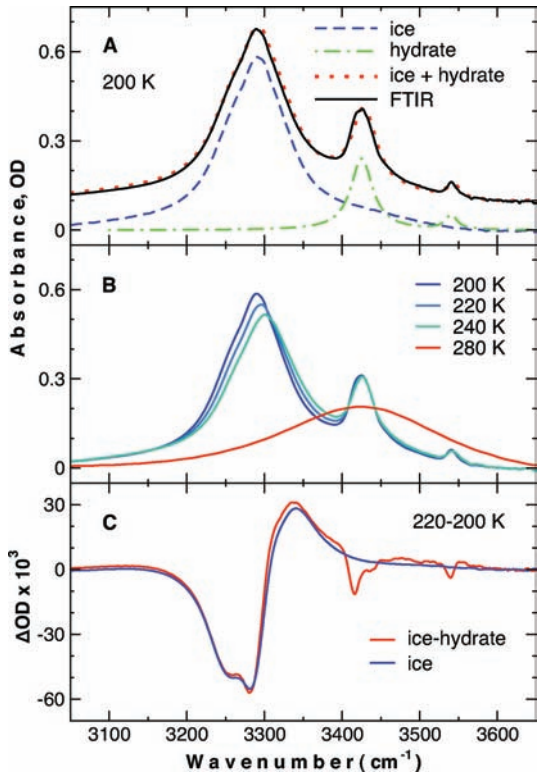

Figure 2. Conventional spectroscopy of NaCl in HDO:D_2O: (A) FTIR spectrum at 200 K (black curve) is represented by the sum of a pure HDO:D_2O ice spectrum scaled by 0.8 (blue dashed line) and two Lorentz curves (green dash-dotted line). The latter are attributed to the OH oscillators in the hydrate crystal structure. The calculated curve (red dotted line) and the measured spectrum are shifted by 0.1 for a better view. (B) FTIR spectra measured at various temperatures in the range from 200 to 280 K. (C) Absorption change measured by increasing the sample temperature from 200 to 220 K in pure ice (blue) and ice-hydrate mixture (red). The ice spectrum of the neat solvent is again scaled by a factor of 0.8.

the ice component shows a distinct, almost linear change of the amplitude and position of the absorption maximum with temperature, whereas its spectral shape remains almost the same.[49] In contrast, both hydrate vibrations appear to be almost unaffected by the temperature change. However, the absorption increase at 3426 and 3541 cm^{-1} due to the temperature shift of the ice component should be considered. The thermal differential spectra for a temperature jump of 20 K are shown in Figure 2C for an ice−hydrate mixture and pure ice in red and blue, respectively. The ice spectrum is again scaled by a factor of 0.8 for easier comparison. The figure shows that both samples have almost the same signature of the thermal differential spectra in the ice region, and differ in the regions around 3426 and 3541 cm^{-1}.

The simple temperature dependence allows the determination of transient temperature jumps in the sample by fitting steady-state thermal differential spectra to the measured time-resolved data.[50] However, the laser induced temperature jump occurs at almost constant volume, leading to a simultaneous pressure increase. Taking into account the isochoric character of the process, we were able to observe ultrafast superheating and melting of bulk ice.[49,50] Melting can be accounted for in the analysis of the transient spectra as well, simply by including a fraction of the liquid FTIR spectrum in the fit.[50] From the data presented in Figure 2 it is evident that both phases can be treated independently in the data analysis of the transient spectra (see below).

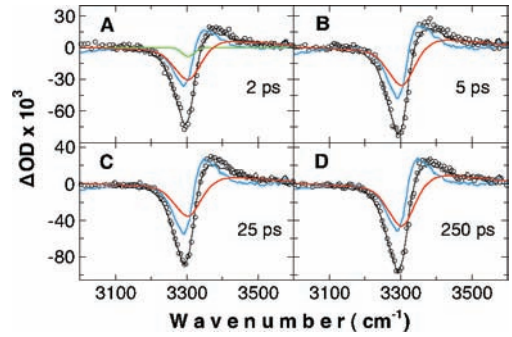

Figure 3. Transient spectra of the crystalline NaCl−HDO:D_2O sample measured after excitation at 3290 cm^{-1}, initial temperature 248 K. Experimental points, calculated solid lines. The black curves are superpositions of the absorption of heated pure ice (blue) and molten liquid (red).

Transient Spectroscopy

We now turn to the time-resolved experiments conducted on NaCl−HDO:D_2O samples in the solid state. Figure 3 shows the time-resolved data measured after excitation of the ice component in the sample. The absorption changes induced by pumping in the maximum of the OH band at 3290 cm^{-1} are recorded for various delay times (see inset). The relaxation of the initially excited OH oscillators (data not shown here) is below 0.5 ps.[51] The spectral signature of the time-resolved data and their temporal evolution are identical (within the experimental resolution) with similar data measured in pure ice.[50] The finding shows that the ice and the hydrate components of the sample are well separated.

The spectra in Figure 3 are analyzed in terms of a temperature jump and partial melting of the ice component in the sample, indicated by the blue and red lines, respectively. The fitting procedure used in the data analysis was described in more detail elsewhere.[50] The small green peak in Figure 3A is attributed to a coherent pump−probe artifact.[52] The good agreement between the calculated thermal differential spectra (black curves) and the transient data should be noted. The temperature jump determined 250 ps after the excitation (see Figure 3D) is 26 ± 3 K, with simultaneous partial melting of the ice crystals of 17 ± 2%. No heating of the hydrate occurs in the measurements, since the feature at 3426 cm^{-1}, seen in Figure 4, is missing. The heat dissipation from the excited ice component can be estimated from the temporal evolution of the absorption changes measured at 3300 cm^{-1} (data not shown). Assuming an exponential decay, the time constant is estimated to be 3 ± 1 ns, consistent with estimations of the heat conduction to the cell windows.[45]

The spectral response should change when pumping the OH groups bonded in the hydrate. For this purpose the pump pulse is tuned to the peak at 3426 cm^{-1}, which is solely attributed to the NaCl hydrate. Due to the residual absorption in the wing of the ice band both phases are pumped and, thus, subject to heating. Because of the lower absorption in this spectral range the amplitude of the pump pulse used here was higher than that in Figure 3. The time-resolved spectra measured at various delay times from 0 to 250 ps are presented in Figure 4A−F. The transient dynamics include the fast population relaxation of the initially excited OH stretching vibration, whereas the long time absorption changes are due to subsequent heating of the both components in the sample. Note the good agreement between the fitted spectra (black) and the experimental data.

The initial dynamics possess three well separated spectral bands centered at 3180, 3290, and 3426 cm^{-1} (see Figure

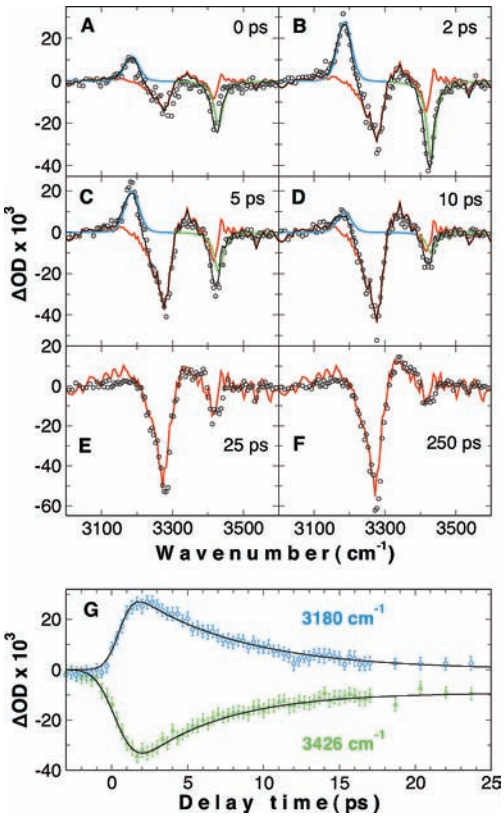

Figure 4. Time-resolved data for solid NaCl−HDO:D_2O with an initial temperature of 200 K after excitation at 3426 cm^{-1}. (A)−(F) Transient spectra taken at various delay times; experimental points, calculated solid lines. The fitted spectra (black curves) are superpositions of thermal differential spectra of the ice-hydrate mixture (red), whereas the green and blue lines represent the population dynamics in the hydrate. (G) Signal transients measured for the maximum of the induced absorption at 3180 cm^{-1} (blue) and bleaching of the OH stretching vibration in the hydrate at 3426 cm^{-1} (green).

4A−C). The maxima of the induced absorption at 3180 cm^{-1} and of the bleaching at 3426 cm^{-1} are reached 2 ps after the excitation. The further development of both features is governed by a simultaneous decay with a time constant of several picoseconds. For longer delays the bleaching at 3426 cm^{-1} reaches an almost constant value, whereas the absorption peak at 3180 cm^{-1} fully disappears for delay times beyond 25 ps (see Figure 4E).

The decrease in optical density at the pump frequency (3426 cm^{-1}) reflects the depletion of the ground state of the excited stretching vibration, with subsequent (partial) ground-state recovery. The latter is accounted for in Figure 4A−D by the green Lorentzian curve centered at 3426 cm^{-1}. The first excited state of the vibration is populated, allowing anharmonically shifted excited-state absorption at 3180 cm^{-1}. The process is represented in Figure 4A−D by the blue Lorentzian peak at 3180 cm^{-1}.

The broad absorption minimum around 3290 cm^{-1} in Figure 4 increases continuously within the first 25 ps and remains almost constant in the next 250 ps. The feature shows the same shape and dynamics as the corresponding bleaching in Figure 3. Therefore, it is attributed to direct excitation of the ice monocrystals in the sample. The transient dynamics of the OH stretching vibration in pure ice is significantly faster than that in the NaCl−hydrate. Thus only the subsequent heating of the ice crystals is included in the data analysis. The red lines in Figure 4 represent the corresponding thermal differential spectra. The additional, smaller feature around 3426 cm^{-1} accounts for the heating of the hydrate, and the red curve in this region stems solely from the Lorentzian difference spectra, as discussed in the previous section. The extracted temperature jump of the ice component in the sample is 17 ± 4 K. The weaker temperature dependence of the hydrate band around 3426 cm^{-1} does not allow a precise determination of the temperature jump induced in the hydrate monocrystals.

The temporal evolution of the OH ground-state bleaching at 3426 cm^{-1} and of its excited-state absorption at 3180 cm^{-1} is depicted in Figure 4G in green and blue, respectively. Both features decay with the same time constant of 6.8 ± 1 ps, which obviously represents the lifetime of the OH stretching vibration in the hydrate. It is an order of magnitude longer than the lifetime of the OH stretching vibration in ice.[51] The finding facilitates the investigation of the dynamics of OH stretching vibration in hydrates with sufficient temporal and spectral resolution.

Conclusions

In this work we present the time-resolved study of the OH stretching vibration in NaCl dihydrate using two-color IR spectroscopy. The hydrate formation is characterized by conventional FTIR measurements. The steady-state spectra of several hydrates are presented. The data give evidence that a polycrystalline ice−hydrate mixture is formed in the samples. The water molecules bound in the NaCl hydrate display two well separated absorption bands at 3426 and 3541 cm^{-1}, respectively. The findings are included in the analysis of the time-resolved data. The transient response on pumping the ice component in the sample at 3290 cm^{-1} agrees with ultrafast heating of pure ice studied previously.[49,50] After 250 ps no significant heating of the hydrate component observed via excitation of the ice component.

The relaxation time of the stronger OH stretching vibration in the NaCl dihydrate at 3426 cm^{-1} is measured to be 6.8 ± 1 ps. The decay is an order of magnitude slower than in water or pure ice. Conclusions on the relaxation pathway of the OH stretching vibration cannot be drawn from these measurements alone but the isolated positioning of the excited OH oscillators in the hydrate crystal implies a smaller density of states that can serve as accepting modes in the transient relaxation of the stretching vibration, which is in accordance with the long lifetime of the latter in the hydrate crystal.

The hydrate crystals represent a model system for the investigation of the transient relaxation of the stretching vibration in hydrogen bonded systems. Since a variety of different hydrates can be prepared with our technique, we consider the hydrates to be promising candidates for further systematic investigations. An expansion of the investigation to other hydrates will offer new insights into the physics underlying the detection of hydrogen bonded systems via the OH group and should be pursued experimentally and theoretically.

Acknowledgment. We thank Prof. Alfred Laubereau for the helpful discussions and continuous support during the whole investigation. This work was supported by the DFG Cluster of Excellence "Munich Center for Advanced Photonics". J.C.W. thanks the International Max Plank Research School on Advanced Photon Science for financial support.

References and Notes

(1) Cleland, W. W.; Kreevoy, M. M. Low-barrier hydrogen bonds and enzymic catalysis. *Science* **1994**, *264*, 1887–1890.

(2) Fersht, A. R.; Shi, J.-P.; Knill-Jones, J.; Lowe, D. M.; Wilkinson, A. J.; Blow, D. M.; Brick, P.; Carter, P.; Waye, M. M. Y.; Winter, G. Hydrogen bonding and biological specificity analysed by protein engineering. *Nature* **1985**, *314*, 235–238.

(3) Baker, E. N.; Hubbard, R. E. Hydrogen bonding in globular proteins. *Prog. Biophys. Mol. Biol.* **1984**, *44* (2), 97–179.

(4) Franks, F. *Water: A comprehensive Treatise*; Plenum Press: New York, 1972.

(5) Hadzi, D. Theoretical Treatments of Hydrogen Bonding. *Wiley Research Series in Theoretical Chemistry*; Wiley: New York, 1997.

(6) Eisenberg, D.; Kauzmann, W. *The Structure and Properties of Water*; Oxford University Press: Oxford, U.K., 1969.

(7) Nibbering, E. T. J.; Elsaesser, T. H. Ultrafast vibrational dynamics of hydrogen bonds in the condensed phase. *Chem. Rev.* **2004**, *104*, 1887–1914.

(8) Graener, H.; Seifert, G.; Laubereau, A. New spectroscopy of water using tunable picosecond pulses in the infrared. *Phys. Rev. Lett.* **1991**, *61*, 2092–2095.

(9) Laenen, R.; Rauscher, C.; Laubereau, A. Dynamics of local substructures in water observed by ultrafast infrared hole burning. *Phys. Rev. Lett.* **1998**, *80*, 2622–2625.

(10) Woutersen, S.; Emmerichs, U.; Bakker, H. J. Femtosecond mid-ir pump-probe spectroscopy of liquid water: Evidence for a two-component structure. *Science* **1997**, *278*, 658–660.

(11) Lindner, J.; Vöhringer, P.; Pshenichnikov, M. S.; Cringus, D.; Wiersma, D. A.; Mostovoy, M. Vibrational relaxation of pure liquid water. *Chem. Phys. Lett.* **2006**, *421* (4), 329–333.

(12) Fecko, C. J.; Eaves, J. D.; Loparo, J. J.; Tokmakoff, A.; Geissler, P. Ultrafast hydrogen-bond dynamics in the infrared spectroscopy of water. *Science* **2003**, *301*, 1698–1702.

(13) Dlott, D. D. Vibrational energy redistribution in polyatomic liquids: 3D infrared-Raman spectroscopy. *Chem. Phys.* **2001**, *266*, 149–166.

(14) Bakker, H. J.; Elsaesser, T. H. *Ultrafast Hydrogen Bonding Dynamics and Proton Transfer Processes in the Condensed Phase*, 1st ed.; Springer-Verlag Gmbh: Berlin, 2002.

(15) Leetmaa, M.; Wikfeldt, K. T.; Ljungberg, M. P.; Odelius, M.; Swenson, J.; Nilsson, A.; Pettersson, L. G. M. Diffraction and IR/Raman data do not prove tetrahedral water. *J. Chem. Phys.* **2008**, *129*, 084502−13.

(16) Walrafen, G. E.; Hokmabadi, M. S.; Yang, W.-H. Raman isosbestic points from liquid water. *J. Chem. Phys.* **1986**, *85*, 6964.

(17) Smith, J. D.; Cappa, C. D.; Wilson, K. R.; Cohen, R. C.; Geissler, P. L.; Saykally, R. J. Unified description of temperature-dependent hydrogen-bond rearrangements in liquid water. *Proceedings of the National Academy of Sciences* **2005**, *102*, 14171–14174.

(18) Emsley, J. W.; Feeney, J.; Sutcliffe, L. H. *Progress in NMR spectroscopy*; Pergamon: New York, 1969.

(19) Morgan, J.; Warren, B. E. X-ray analysis of the structure of water. *J. Chem. Phys.* **1938**, *6*, 666.

(20) Narten, A. H.; Levy, H. A. Observed diffraction pattern and proposed models of liquid water. *Science* **1969**, *165*, 3892.

(21) Soper, A. K. The quest for the structure of water and aqueous solutions. *J. Phys.: Condens. Matter* **1997**, *9* (13), 2717–2730.

(22) Wernet, Ph.; Nordlund, D.; Bergmann, U.; Cavalleri, M.; Odelius, M.; Ogasawara, H.; Näslund, L.; Hirsch, T. K.; Ojamäe, L.; Glatzel, P.; Pettersson, L. G. M.; Nilsson, A. The structure of the first coordination shell in liquid water. *Science* **2004**, *304*, 995–999.

(23) Rey, R.; Moller, K. B.; Hynes, J. T. Ultrafast vibrational population dynamics of water and related systems: A theoretical perspective. *Chem. Rev.* **2004**, *104*, 1915–1928.

(24) Stenger, J.; Madsen, D.; Hamm, P.; Nibbering, E. T. J.; Elsaesser, T. H. A photon echo peak shift study of liquid water. *J. Phys. Chem. A* **2002**, *106*, 2341–2350.

(25) Ashbury, J. B.; Steinel, T.; Kwak, K.; Corcelli, S. A.; Lawrence, C. P.; Skinner, J. L.; Fayer, M. D. Dynamics of water probed with vibrational echo correlation spectroscopy. *J. Chem. Phys.* **2004**, *121*, 12431.

(26) Mancinelli, R.; Botti, A.; Bruni, F.; Ricci, M. A.; Soper, A. K. Perturbation of water structure due to monovalent ions in solution. *Phys. Chem. Chem. Phys.* **2007**, *9*, 2959–2967.

(27) Kropman, M. F.; Bakker, H. J. Dynamics of water molecules in aqueous solvation shells. *Science* **2001**, *291*, 2118–2120.

(28) Laenen, R.; Thaller, A. Water in the vicinity of solvated ions: modified dynamical and structural water properties resolved by sub-picosecond ir-spectroscopy. *Chem. Phys. Lett.* **2001**, *349*, 442–450.

(29) Bakker, H. J. Structural dynamics of aqueous salt solutions. *Chem. Rev.* **2008**, *108*, 1456–1473.

(30) Jungwirth, P.; Tobias, D. J. Specific ion effects at the Air/Water interface. *Chem. Rev.* **2006**, *106* (4), 1259–1281.

(31) Auer, B. M.; Skinner, J. L. Ir and raman spectra of liquid water: Theory and interpretation. *J. Chem. Phys.* **2008**, *128*, 224511.

(32) Kuharski, R. A.; Rossky, P. J. Quantum mechanical contributions to the structure of liquid water. *Chem. Phys. Lett.* **1984**, *103*, 357–362.

(33) Kühne, T. D.; Krack, M.; Parrinello, M. Static and dynamical properties of liquid water from first principles by a novel Car-Parrinello-like approach. *J. Chem. Theory Comput.* **2009**, *5* (2), 235–241.

(34) Bukowski, R.; Szalewicz, K.; Groenenboom, G. C.; van der Avoird, A. Predictions of the properties of water from first principles. *Science* **2007**, *315* (5816), 1249–1252.

(35) Xenides, D.; Randolf, B. R.; Rode, B. M. Structure and ultrafast dynamics of liquid water: A quantum mechanics/molecular mechanics molecular dynamics simulations study. *J. Chem. Phys.* **2005**, *122* (17), 174506–10.

(36) Bukowski, R.; Szalewicz, K.; Groenenboom, G. C.; van der Avoird, A. Polarizable interaction potential for water from coupled cluster calculations. II. applications to dimer spectra, virial coefficients, and simulations of liquid water. *J. Chem. Phys.* **2008**, *128* (9), 094314−20.

(37) Schmidt, J. R.; Roberts, S. T.; Loparo, J. J.; Tokmakoff, A.; Fayer, M. D.; Skinner, J. L. Are water simulation models consistent with steady-state and ultrafast vibrational spectroscopy experiments? *Chem. Phys.* **2007**, *341*, 143–157.

(38) Auer, B. M.; Skinner, J. L. IR and raman spectra of liquid water: Theory and interpretation. *J. Chem. Phys.* **2008**, *128*, 224511–12.

(39) Fanourgakis, G. S.; Xantheas, S. S. Development of transferable interaction potentials for water. v. extension of the flexible, polarizable, thole-type model potential (TTM3-F, v. 3.0) to describe the vibrational spectra of water clusters and liquid water. *J. Chem. Phys.* **2008**, *128* (7), 074506−11.

(40) Fanourgakis, G. S.; Xantheas, S. S. The bend angle of water in ice ih and liquid water: The significance of implementing the nonlinear monomer dipole moment surface in classical interaction potentials. *J. Chem. Phys.* **2006**, *124* (17), 174504–4.

(41) Vaniman, D. T.; Bish, D. L.; Chipera, S. J.; Fialips, C. I.; Carey, J. W.; Feldman, W. C. Magnesium sulphate salts and the history of water on mars. *Nature* **2004**, *431*, 663–665.

(42) Pandey, A.; Webb, C.; Soccol, C. R.; Larroche, C. *Enzyme technology*; Springer: Berlin, 2006.

(43) Lutz, H. D. Structure and strength of hydrogen bonds in inorganic solids. *J. Mol. Struct.* **2003**, *646* (1−3), 227–236.

(44) Lutz, H. D.; Jung, C. Water molecules and hydroxide ions in condensed materials; correlation of spectroscopic and structural data. *J. Mol. Struct.* **1997**, *404*, 63–66.

(45) Schmeisser, M.; Thaller, A.; Iglev, H.; Laubereau, A. Picosecond temperature and pressure jumps in ice. *New J. Phys.* **2006**, *8*, 104.

(46) Lutz, H. D. *Bonding and structure of water molecules in solid hydrates. Correlation of spectroscopic and structural data*; Springer: Berlin/Heidelberg, 1988; pp 97−125.

(47) Novak, A. *Hydrogen bonding in solids correlation of spectroscopic and crystallographic data*; Springer Berlin/Heidelberg: 1974; pp 177−216.

(48) Klewe, B.; Pedersen, B. Crystal structure of sodium-chloride dihydrate. *Acta Crystallogr. Sect. B - Struct. Sci.* **1974**, *B 30*, 2363–2371.

(49) Iglev, H.; Schmeisser, M.; Simeonidis, K.; Thaller, A.; Laubereau, A. Ultrafast superheating and melting of bulk ice. *Nature* **2006**, *439*, 183–186.

(50) Schmeisser, M.; Iglev, H.; Laubereau, A. Bulk melting of ice at the limit of superheating. *J. Phys. Chem. B* **2007**, *111*, 11271–11275.

(51) Woutersen, S.; Emmerichs, U.; Nienhuys, H. K.; Bakker, H. J. Anomalous temperature dependence of vibrational lifetimes in water and ice. *Phys. Rev. Lett.* **1998**, *81*, 1106.

(52) Laenen, R.; Rauscher, C. Numerical study of induced polarization dynamics in ultrafast spectral hole-burning experiments. *Chem. Phys.* **1998**, *230*, 223.

JP904558M